

**ELECTROWEAK AND TOP PHYSICS RESULTS FROM DØ**PUSHPALATHA C BHAT<sup>†</sup>*Fermi National Accelerator Laboratory  
Batavia, IL 60510, USA**For the DØ Collaboration*

The collider Run II at Fermilab that started in March 2001 with upgraded accelerator complex and detectors is progressing extremely well. An integrated luminosity of 670 pb<sup>-1</sup> was delivered to the CDF and DØ experiments each, by the end of August 2004. Additional planned upgrades to the accelerators will result in an integrated luminosity of 4 - 8 fb<sup>-1</sup> for each experiment by the end of 2009. I present some preliminary electroweak and top quark physics measurements made by the DØ collaboration analyzing data sets corresponding to integrated luminosity in the range of 150-250 pb<sup>-1</sup>.

**1.1. Introduction**

The CDF and DØ experiments, at the Fermilab proton-antiproton collider, have entered a new era in the exploration of physics near the electroweak scale. Already about four times more data than collected in Run I has been accumulated and an order of magnitude more will become available over the next several years, greatly expanding the scope for exploration and discovery with direct searches and with precision measurements of the top and electroweak physics. The excellent performance of the Tevatron and the CDF and DØ experiments during Run I (1992-96) made possible the discovery of the top quark in 1995 [1], which was widely acknowledged as a major triumph of the Standard Model (SM). Other highlights of Run I results include precision measurements of the top quark mass, top-antitop production cross section, W boson mass, rates of a number of SM processes, and searches for possible new physics. The collider Run II started in March 2001 after major upgrades to the accelerator complex and the detectors, and with the higher center of mass energy of  $\sqrt{s}=1.96$  TeV. Additional Run II upgrades [2] underway throughout the accelerator complex are expected to result in 4-8 fb<sup>-1</sup> of data delivered to each of the experiments by 2009. This large data set will allow refined measurements of the top quark and its dynamics and the exploration of the

---

<sup>†</sup> pushpa@fnal.gov

To be published in the proceedings of the 10th international symposium on *Particles, Strings and Cosmology* (PASCOS'04/Nath Fest), Northeastern University, Boston, August 16-22, 2004. (World Scientific)

tantalizing possibility that the top quark plays a role in electroweak symmetry breaking. Precision measurements of electroweak processes and a wealth of other physics are guaranteed and the potential for discoveries is great.

Both the CDF and DØ detectors underwent major upgrades in preparation for Run II. The Run II DØ detector [3] has three major sub-systems - a new central tracking system, comprising a Silicon Microstrip Tracker (SMT) and a Central Fiber Tracker (CFT) inside a 2T solenoidal magnetic field, a Uranium/liquid-Argon calorimeter surrounding the central tracker and an upgraded outer muon spectrometer. Fig. 1 shows a photograph of the assembled detector in the collision hall and Fig. 2 shows the schematic drawings of the full detector and the central tracking system. The SMT has six concentric barrels of four layers each, nested around the beam pipe, interspersed with twelve radial disks and, additionally, 4 large radial disks at large  $z$  along the beam axis, collectively providing a coverage in the pseudorapidity range of  $|\eta| < 3$ , (where  $\eta = -\ln(\tan \theta/2)$  and  $\theta$  is the polar angle). The CFT has eight coaxial barrels, each supporting two doublets of overlapping scintillating fibers, one doublet parallel to the beam axis and the other alternating by  $\pm 3^\circ$  relative to the beam axis. The calorimeter has three parts - a central calorimeter (CC) up to  $|\eta| \sim 1.1$  and two end calorimeters (EC) extending the coverage to  $|\eta| \sim 4.2$ , each housed in a separate cryostat. To aid in particle identification, each calorimeter consists of an inner electromagnetic (EM) section, a fine hadronic (FH) section and a coarse hadronic (CH) section. The absorber in the EM and FH sections is depleted Uranium; in the CH section, it is a mixture of stainless steel and copper. Scintillators between the CC and EC cryostats provide sampling of showers for  $1.1 < |\eta| < 1.4$ . The muon system consists of a layer of drift chambers for tracking and scintillation trigger counters in front of magnetized iron toroids, with a magnetic field of 1.8 T and two similar layers behind the toroids. Tracking in the muon system for  $|\eta| < 1$  uses 10 cm wide drift tubes while 1 cm mini drift tubes are used in the forward muon system for  $1 < |\eta| < 2$ .

The online trigger system that selects events for storage and offline analysis has three levels. The first two levels are implemented in hardware and firmware and the third level is primarily implemented in software running on a parallel processing farm of commodity CPUs. Candidates for tracks, electrons, jets, muons and missing energy are formed using information from individual detectors at Level 1, then processed and combined with increasing sophistication, in the higher level systems. Data at Level-3 are written to mass storage at the rate of 50 to 60 Hz.

The accelerator performance has improved significantly in the past year as a direct result of many reliability and operational improvements and upgrades [2]. The integrated luminosity delivered by the Tevatron so far, during Run II, to the experiments is about  $670 \text{ pb}^{-1}$  of which DØ has recorded about  $460 \text{ pb}^{-1}$  with a

fully operational Run II detector. It is expected that  $2 \text{ fb}^{-1}$  will be delivered by mid-2006,  $\sim 4 \text{ fb}^{-1}$  by 2007 and in excess of  $8 \text{ fb}^{-1}$  by 2009. Of the  $460 \text{ pb}^{-1}$  data collected so far, the electroweak and top physics results reported here come from analyses of data corresponding to  $150 - 250 \text{ pb}^{-1}$ .



Figure 1. Photograph of the DØ detector in the collision hall, prior to the start of Run I.

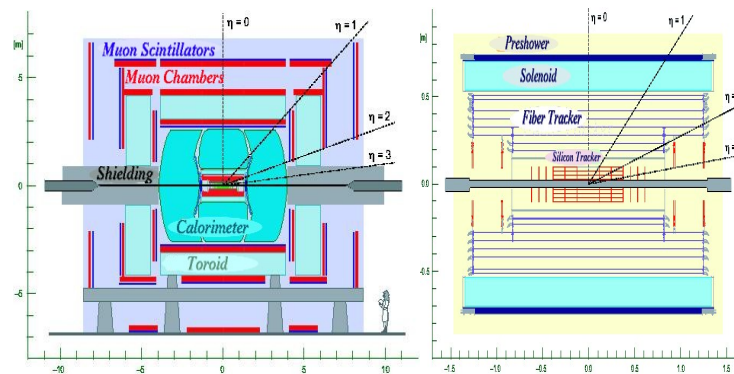


Figure 2. Schematic drawings of (Left) the full detector showing the three major sub-systems: the Central Tracker, the central and end-cap Calorimeters and the Muon system and (right) the components of the central tracking system. See text for details.

## 1.2. Measurements with Electroweak Bosons

Rigorous studies of the electroweak gauge bosons, W and Z, and the processes containing them are of paramount importance for a variety of reasons. The W boson mass is an important standard model parameter and, together with the top quark mass, constrains the mass of the SM Higgs boson. The production rates of the W and Z bosons and the di-boson states WW, WZ and ZZ provide stringent tests of the electroweak Standard Model and Quantum Chromodynamics (QCD). A comparison of the leptonic branching fractions  $B(W \rightarrow \ell\nu)$ , where  $\ell = e, \mu$ , or  $\tau$ , tests the universality of leptonic couplings to the weak current. The angular distributions of leptons from W boson decay provides constraints on ratios of parton distribution functions (PDF) of the proton and will yield better understanding of the next-to-leading order (NLO) corrections to the production models. The W and Z bosons are present in the final states of many interesting physics processes that are the prime objects of study, such as the decay products of the top quark and in associated production with the, yet to be discovered, Higgs boson. The SM processes involving the production of electroweak bosons also form important backgrounds to searches for new physics. Large W and Z boson samples provide excellent calibration tools for the detector energy scale and to benchmark the performance of the detector, trigger, and event reconstruction algorithms. The W boson production can also be used to calibrate the luminosity measurement for the experiments.

### 1.2.1. W and Z Boson Production Cross Sections

Hadronic decays of the W and Z bosons are difficult to measure due to large backgrounds from QCD jet production. Therefore, W and Z bosons are mainly identified and measured in the leptonic decay channels. The W and Z production cross sections times their branching fraction into leptonic channels ( $\sigma_W \cdot B(W \rightarrow \ell^+ \nu)$  and  $\sigma_Z \cdot B(Z \rightarrow \ell^+ \ell^-)$ , where  $\ell$  is a charged lepton) can be measured with great precision. These measurements provide tests of the QCD predictions for W and Z production. The ratio, R, of these cross section measurements, can be used to measure indirectly the width of the W boson.

The W boson decays are identified by a high transverse energy charged lepton and large transverse missing energy due to the neutrino, while the Z boson events are characterized by two high transverse energy charged leptons. In this paper, we present results from W decays in the electron and muon channels and Z decays in electron, muon and tau channels. The tau channel is particularly interesting because it can be gainfully exploited in searches for the Higgs boson and Supersymmetry (SUSY).

Electrons are identified as electromagnetic (EM) clusters in the calorimeter using a simple cone algorithm. To suppress backgrounds from QCD jet events (jets faking electrons), electron candidates are required to have a large fraction

of their energy (typically >90%) deposited in the EM section of the calorimeter and satisfy certain isolation and cluster shape criteria. Electron candidates are classified as *tight* electrons if a track in the central detector is matched spatially to the EM cluster and if the track momentum is close to the transverse energy of the EM cluster. The W event sample is selected by requiring one central ( $|\eta| < 1.0$ ) electron with transverse energy  $E_T > 25$  GeV and missing transverse energy  $E_T > 25$  GeV. The Z boson sample is selected requiring two *tight* central electrons with  $E_T > 25$  GeV. The transverse mass distribution of the W candidate events and the invariant mass of the two electrons from the Z candidates are shown in Fig. 3, compared with simulations using PYTHIA [4] for signal event generation and a parameterized Monte Carlo model of the detector response.

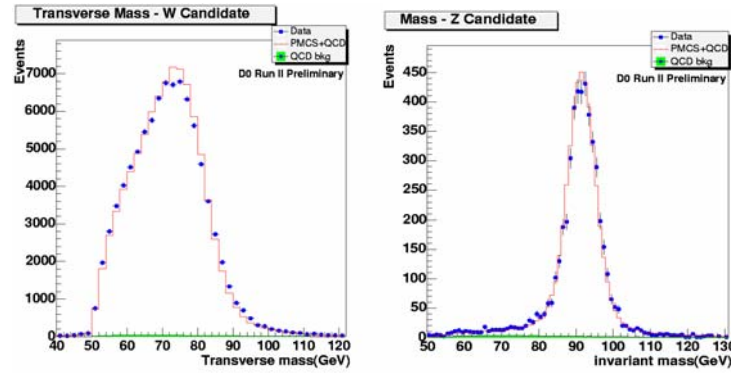


Figure 3. (Left) Transverse mass distribution of W bosons decaying into an electron and a neutrino. (Right) Invariant mass of Z bosons in the di-electron channel. ( $\int L \cdot dt = 177 \text{ pb}^{-1}$ )

Muons are identified as tracks in the outer muon system, matched to tracks in the central tracking system. Muons from the decays of heavy-flavor hadrons form a significant background to the vector boson events in the muon channel. This background is significantly reduced by requiring the muons to be isolated spatially from other objects in the event. Contamination from cosmic ray muons is reduced with criteria on the timing of the signal in the muon chambers relative to the  $p\bar{p}$  interaction time and the impact parameter of the track at the vertex.

The W sample in the muon channel is selected by requiring an isolated muon with transverse momentum  $p_T > 15$  GeV and  $|\eta| < 2.0$ . The Z sample is selected by requiring two oppositely charged, isolated, muons with  $p_T > 15$  GeV and  $|\eta| < 1.8$ . To reduce the background from semi-leptonic b decays, a number of isolation criteria are applied. These include (1) the sum of  $p_T$  of other tracks within a cone of radius  $R=0.5$  (where  $R = \sqrt{(\Delta\eta)^2 + (\Delta\phi)^2}$ ,  $\phi$  being the azimuth) of the candidate muon be less than 3.5 GeV and (2) the total energy

deposition in the calorimeter cells, within a radius of  $R=0.4$ , excluding that of the muon, be less than 2.5 GeV. The invariant mass distribution of the 14352 di-muon candidates coming primarily from Z bosons is shown in Fig.4. The major physics backgrounds for this channel come from b-pairs (estimated to be  $(0.5\pm 0.3)\%$ ),  $Z\rightarrow\tau\tau$  ( $0.5\pm 0.1\%$ ), and  $WW+\text{jets}$  ( $0.2\pm 0.1\%$ ).

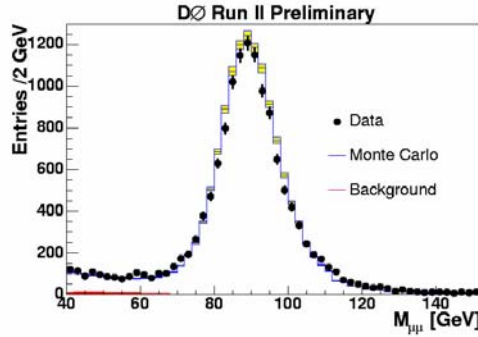


Figure 4. The invariant mass of the di-muons from the Z candidate sample. ( $\int L \cdot dt = 148 \text{ pb}^{-1}$ ).

Identification of  $\tau$  leptons is challenging at a hadron collider. Unlike electrons or muons, the taus decay very close to where they are formed (with a decay length about 4 times smaller than that of the b-quarks) and have to be reconstructed using their decay products. The  $\tau$  identification used in the current analysis is based on the use of neural networks to discriminate 1-prong and 3-prong decays of taus from other sources, and is optimized for the  $Z\rightarrow\tau\tau$  process.

The  $Z\rightarrow\tau\tau$  event selection requires a  $\tau$  candidate (identified as  $\tau\rightarrow\text{hadrons}$  or  $\tau\rightarrow e\nu_e\nu_\tau$ ) back to back with a single isolated muon (from  $\tau\rightarrow\mu\nu_\mu\nu_\tau$ ). Most of the neural network variables are ratios of the energies of various objects (and their sums) to the  $E_T$  of the  $\tau$ , in order to minimize the dependence on  $E_T$ . The isolated muon is required to have a  $p_T > 12$  GeV and the  $\tau$  candidate  $p_T > 5-10$  GeV, depending on the type of decay. The 1946 events selected have an estimated background of 55% from b-quark pairs,  $W+\text{jets}$  and  $Z\rightarrow\mu\mu$ . Fig. 5 shows the invariant mass distribution of the  $\mu$  and  $\tau$  tracks for the background (estimated from the like-sign data sample) and for data (from opposite sign sample and background subtracted) compared with  $Z\rightarrow\tau\tau$  monte carlo.

The cross section times the branching fraction measurements for all channels discussed above are summarized in Table 1. In the Z channels, they are after subtraction of the virtual photon exchange process. The main systematic uncertainty in the measurements is from the luminosity measurement and is about 6%, and is shown separately from other systematic errors. The PDF

uncertainties are typically about 2% and estimated for CTEQ6M PDFs. The contribution from lepton identification is  $\sim 2\%$ . This error is expected to reduce with higher data statistics.

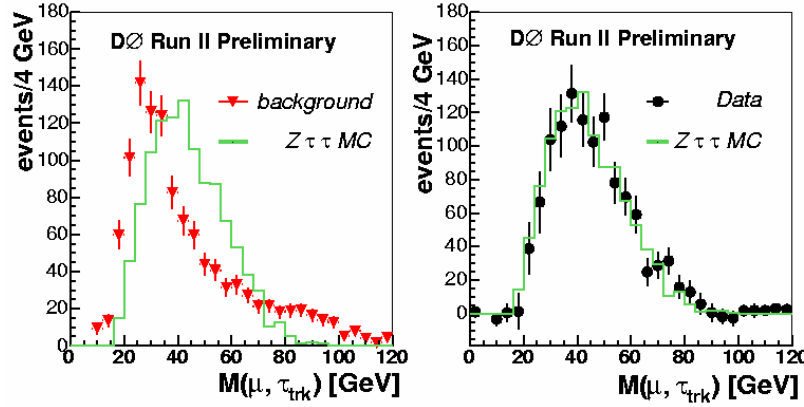


Figure 5. Invariant mass distribution of the  $\mu$  and  $\tau$  tracks for background sample using like-sign tracks (left) and for Z candidate data with opposite sign tracks (right) for the  $Z \rightarrow \tau\tau$  process shown normalized to  $Z \rightarrow \tau\tau$  monte carlo. The data sample corresponds to  $\int \mathcal{L} \cdot dt = 207 \text{ pb}^{-1}$ .

Table 1. W and Z boson inclusive cross sections in various leptonic decay channels.

Channel	Number of Candidates	Bkg. (%)	$\int \mathcal{L} dt$ ( $\text{pb}^{-1}$ )	$\sigma \cdot B$ (pb)
$W \rightarrow e\nu$	116569	3.15	177	$2865 \pm 8.3(\text{stat}) \pm 74.7(\text{sys}) \pm 186.2(\text{lum})$
$W \rightarrow \mu\nu$	8305	11.8	17	$3226 \pm 128(\text{stat}) \pm 100(\text{sys}) \pm 323(\text{lum})$
$Z \rightarrow e^+e^-$	4712	1.8	177	$264.9 \pm 3.9(\text{stat}) \pm 9.9(\text{sys}) \pm 17.2(\text{lum})$
$Z \rightarrow \mu^+\mu^-$	14352	1.4	148	$291.3 \pm 3.0(\text{stat}) \pm 6.9(\text{sys}) \pm 18.9(\text{lum})$
$Z \rightarrow \tau^+\tau^-$	1946	55	207	$256 \pm 16(\text{stat}) \pm 17(\text{sys}) \pm 16(\text{lum})$

The measured cross sections are in good agreement with theoretical calculations as shown in Fig. 6. The ratio of the leptonic W and Z cross sections is much more precisely determined than the individual cross sections because the largest systematic uncertainty due to luminosity measurement cancels. This ratio, in the electron channel, is measured to be  $R = 10.82 \pm 0.16(\text{stat}) \pm 0.28(\text{sys})$ .

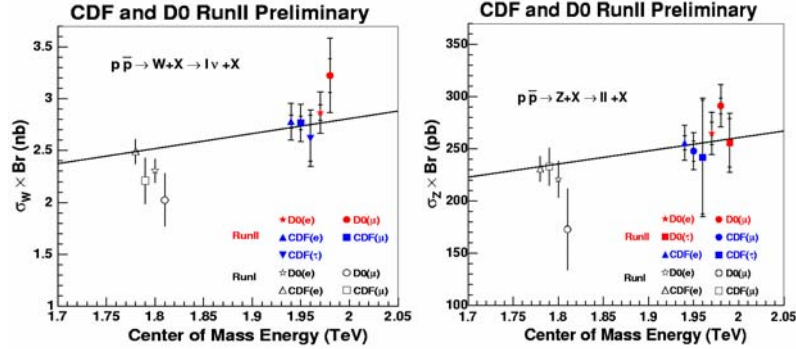


Figure 6. W and Z boson cross section measurements in all leptonic channels from Run II (preliminary) and Run I, from CDF and DØ, compared with NNLO (next-to-next leading order) theoretical predictions.

### 1.2.2. Di-boson Production Cross Sections

Studies of multiple electroweak boson production at the Tevatron can help probe the gauge structure of the SM and search for anomalous couplings. Trilinear gauge couplings larger than those predicted by the SM may signal new physics. The di-boson production processes are also important backgrounds in many new particle searches and therefore need to be understood and measured well.

The WW production has been studied in ee, e $\mu$  and  $\mu\mu$  channels, using data sets corresponding to luminosities in the range of 220-250 pb<sup>-1</sup>. In the ee and  $\mu\mu$  channels, one of the important backgrounds is due to Z bosons. The dominant background in the ee channel is from W+jet events where a hadronic jet can fake an electron. The e $\mu$  channel is the cleanest of all, with a signal to background ratio of about 4. Combining all three channels, we expect 16.1 $\pm$ 0.1 events from WW production and 8.05 $\pm$ 0.70 events from background sources.

With 25 events found in data, a cross section of 13.8<sup>+4.3</sup><sub>-3.8</sub> (stat)  $\pm$  1.0(sys)  $\pm$  0.9(lum) pb has been measured.

In a search for associated production of WZ events in the trilepton channel (containing electrons and muons), in about 200 pb<sup>-1</sup> of data, we expect to find 1.02 $\pm$ 0.07 signal events and 0.39 $\pm$ 0.02 background events after the selection cuts. One tri-muon candidate event remains in the data. The analysis yields an upper limit of 15.1 pb on the WZ cross section at 95% C.L. The SM prediction is about 3.7 pb.

The associated production of a photon with a W or Z has been studied using W and Z decays in electron and muon channels. Photons are identified as EM clusters in the calorimeters with isolation and cluster shape criteria as in the case of electrons. Photons are distinguished from electrons by the absence of tracks in the central tracker pointing to and consistent with the EM cluster. The sum of  $p_T$  of the tracks within a cone of  $R=0.4$  is required to be less than 3 GeV. The  $p_T$  of the photon is required to be larger than 8 GeV. The dominant background in both channels comes from W/Z + jet events where the jet fakes a photon. This background is determined by measuring the rate for a jet to fake a photon in a sample of QCD multi-jet events and applying it to samples of W/Z + jet events. In the  $W\gamma$  analysis, using  $162 \text{ pb}^{-1}$  of data for the electron channel and  $82 \text{ pb}^{-1}$  of data for the muon channel, 146 and 77 events are observed, with estimated backgrounds of  $87.1 \pm 7.5$  and  $37 \pm 10$ , respectively. In the  $Z\gamma$  analysis using  $117 \text{ pb}^{-1}$  of data in the electron channel and  $144 \text{ pb}^{-1}$  in the muon channel 33 and 68 events are observed, with estimated backgrounds of  $4.7 \pm 0.7$  and  $10.1 \pm 1.3$  events, respectively. Combining the two channels, the cross sections are measured to be  $\sigma(p\bar{p} \rightarrow W\gamma + X \rightarrow \ell\nu\gamma + X) = 19.3 \pm 6.7(\text{stat+sys}) \pm 1.2(\text{lum}) \text{ pb}$  and  $\sigma(p\bar{p} \rightarrow Z\gamma + X \rightarrow \ell\ell\gamma + X) = 3.9 \pm 0.5(\text{stat+sys}) \pm 0.3(\text{lum}) \text{ pb}$ .

### 1.3. Results on Top Quark Production and Properties

The dominant production mechanism for top quarks at a hadron collider is pair production of top and anti-top quarks through the strong interaction processes of quark-antiquark annihilation and gluon-gluon fusion. At the Tevatron, at  $\sqrt{s} = 1.96 \text{ TeV}$ , the relative contributions of these two processes are about 85% and 15%, respectively. The top quarks can also be produced singly, through electroweak processes, but with a rate calculated to be about half of that for pair production. According to the SM, each top quark decays into a W boson and a b-quark, nearly 100% of the time. The  $t\bar{t}$  events are classified into *dilepton*, *lepton + jets* and *all-jets* channels depending on whether one or both of the W bosons decay leptonically or hadronically. The *all-jets* events have the largest branching fraction (~45%) but suffer from huge backgrounds from other QCD multijet events. The *lepton+jets* channels each have a branching fraction of 14.5% for each kind of charged lepton, and the cleanest *dilepton* channel,  $e\mu$ , has ~2.5% while  $ee$  and  $\mu\mu$  have each ~1.2%. In the following sections, we describe the recent results on the top quark cross section measurements in various channels and the measurement of its mass, using a Run II data sample corresponding to  $\int L \cdot dt = 140 - 160 \text{ pb}^{-1}$ .

### 1.3.1 Top-antitop Pair Production Cross Section

Preliminary measurements of the cross section from *dilepton* and *lepton+jets* channels are reported here.

The signature for  $t\bar{t}$  decays in *dilepton* channels is the presence of two high  $E_T$ , central, isolated leptons, two jets initiated by the b-quarks (one or both may be tagged using the SMT) and a large  $E_T$  arising from the two neutrinos. The dominant physics backgrounds are from leptonic decays of the Z, the Drell-Yan process, and vector boson pair production. The instrumental backgrounds arise from mis-measured  $E_T$  in  $Z \rightarrow \ell\ell$  decays and from fake leptons in W+jets events. Candidates were selected by requiring two isolated leptons (electron or muon), with  $E_T > 15$  GeV in  $e\mu$  channel,  $E_T > 20$  GeV in  $ee$  channel and  $|\eta| < 1.1$  or  $1.5 < |\eta| < 2.5$  for electrons and  $p_T > 15$  GeV and  $|\eta| < 2.0$  for muons. At least two jets with  $E_T > 20$  GeV and  $E_T > 25$  GeV for the  $e\mu$  channel and  $E_T > 35$  GeV in the case of  $ee$  and  $\mu\mu$  channel, are required. Events with *dilepton* invariant mass consistent with a Z are removed in the  $ee$  and  $\mu\mu$  channels. To further increase the signal to background ratio, a cut on  $H_T$  (the scalar sum of the transverse energies of the leading lepton and the jets in the event) is imposed.  $H_T$  is required to be larger than 140 GeV in the  $e\mu$  channel and 120 GeV in the  $\mu\mu$  channel. Combining the  $ee$ ,  $e\mu$  and  $\mu\mu$  channels yields 17 observed events, with an expected background of  $4.8 \pm 0.7$  events and signal of  $6.0 \pm 0.5$  events (for  $m_t = 175$  GeV and an assumed  $t\bar{t}$  cross section of 7 pb). This yields a cross section measurement of,  $\sigma_{t\bar{t}} = 14.3_{-4.3}^{+5.1} (\text{stat})_{-1.9}^{+2.6} (\text{sys}) \pm 0.9 (\text{lum}) \text{ pb}$ . A separate analysis has also been performed in the  $e\mu$  channel requiring one of the jets be b-tagged with a reconstructed secondary vertex. This selection is virtually background-free ( $< 0.1$  event); 5 events are observed with an expected signal of 3.2 events, and this results in a measured cross section of  $\sigma_{t\bar{t}} = 11.1_{-4.3}^{+5.8} (\text{stat}) \pm 1.4 (\text{sys}) \pm 0.6 (\text{lum}) \text{ pb}$ .

In the *lepton+jets* channels, where the signature is one high  $p_T$  lepton, large  $E_T$  and four or more jets (2 of which are b-jets), two analysis approaches have been employed. The analyses use  $e$ +jets ( $\mu$ + jets) events with  $E_T^e (p_T^\mu) > 20$  GeV,  $|\eta| < 1.1 (2.0)$ ,  $E_T > 20 (17)$  GeV, four jets with  $E_T > 15$  GeV and  $|\eta| < 2.5$ . As pioneered by DØ in Run I [5], in the so-called ‘‘topological’’ analysis, four variables with good discriminating power between the signal and background are combined into a likelihood discriminant. The variables used here are the event aplanarity, sphericity, a third variable that measures the centrality of the event and a fourth variable that measures the extent to which the jets are clustered together. The discriminant distribution for the data events and results

of fits to signal and backgrounds for the  $e+jets$  channel are shown in Fig. 7 (plot on the left). The measured cross section from combining both channels is,

$$\sigma_{t\bar{t}} = 7.2_{-2.4}^{+2.6} (\text{stat})_{-1.7}^{+1.6} (\text{sys}) \pm 0.5 (\text{lum}) \text{ pb} .$$

An analysis has also been performed using two different b-tagging algorithms: (1) based on the reconstruction of a secondary vertex (SVT) and (2) based on measuring the impact parameter of tracks with respect to the primary interaction vertex (CSIP). The jet multiplicity distributions for data for the single SVT tagged events are shown in Fig. 7 (right plot), and compared with signal and background contributions. These analyses provide the most precise  $t\bar{t}$  cross section measurements from the Run II DØ data and are,

$$\sigma_{t\bar{t}} = 8.2 \pm 1.3 (\text{stat})_{-1.6}^{+1.9} (\text{sys}) \pm 0.5 (\text{lum}) \text{ pb} \text{ from the SVT analysis and}$$

$$\sigma_{t\bar{t}} = 7.2_{-1.2}^{+1.3} (\text{stat})_{-1.4}^{+1.9} (\text{sys}) \pm 0.5 (\text{lum}) \text{ pb} \text{ from the CSIP analysis.}$$

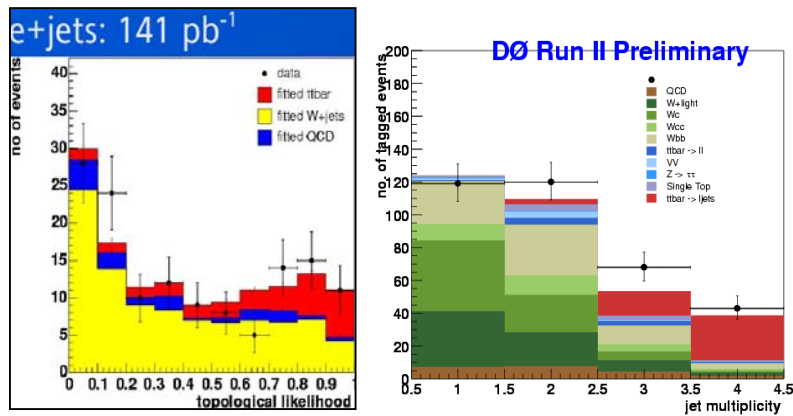


Figure 7. (Left) Distribution of the likelihood discriminant of data events, compared with expected signal and main backgrounds (W+jets and QCD) in the  $electron+jets$  channel from the topological analysis. (Right) Jet multiplicity distribution of single b-tagged events in the  $lepton+jets$  channel. The data bins with jet multiplicity of  $\geq 3$  jets per event show an excess of events above background consistent with expected top-antitop events.

The results of cross section measurements in a variety of final states are summarized in Fig. 8.

### 1.3.2 Top Quark Mass Measurement

The top quark mass was measured with impressive precision in Run I [6]. The latest CDF and DØ combined result for the top mass using Run I data is  $178.0 \pm 4.3$  GeV. That precision will be well surpassed in Run II because of the huge statistics of  $t\bar{t}$  events that will be accumulated. However, for this to

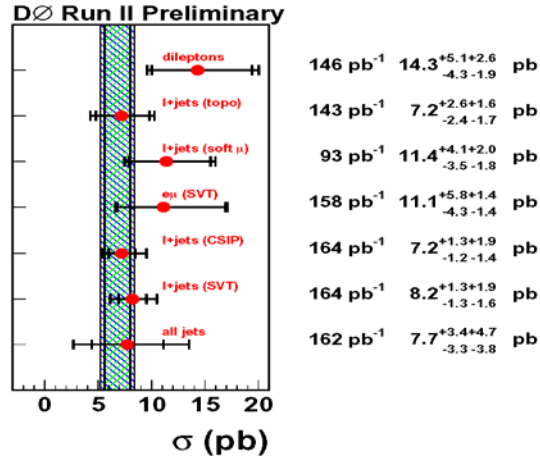


Figure 8. Top pair production cross section measurements using a variety of decay channels. The band shows the predicted theoretical cross section with uncertainties. The luminosity of the data sample used in each case and the cross section with statistical and systematic errors are listed to the right of the plot. The uncertainty from luminosity is about 6%.

happen detailed understanding of the detector energy scale and control of other systematic effects are essential. Preliminary results from two analyses of the *lepton+jets* events using about 160 pb<sup>-1</sup> of data are reported here.

The data sample used is the same as for the topological cross section analysis in the *lepton+jets* channel. A further requirement of  $E_T > 20$  GeV is imposed on the three leading jets. Kinematic fits to the top-antitop hypothesis are performed for candidate events to extract top quark mass information for each event. Since there are 12 possible permutations to assign the four jets in the decay hypothesis, a fitted top quark mass and the fit  $\chi^2$  is obtained for each permutation. Events that have at least one fit with  $\chi^2 < 10$  are retained. To further reduce backgrounds from mis-identified electrons,  $|E_T^\ell| + |E_T| > 65$  GeV is required. A total of 101 e+jets and 90  $\mu$ +jets events pass these criteria; the expected number of signal events is about 30 in each case.

The top quark mass is extracted from this sample using two methods. The first method, called the template method, compares the observed fitted mass distribution (using the lowest  $\chi^2$  solution) with background and signal fitted mass templates (for different possible top masses) to extract the top quark mass. The second method, which is an ideogram technique, extracts the mass

information from a combined likelihood for the sample, taking into account all information in the kinematic fit and the probability for an event to be signal or background, as measured by the event likelihood discriminant similar to that described in section 1.3.1. The top quark mass is measured to be  $m_t = 170 \pm 6.5(\text{stat})_{-6.1}^{+10.5}(\text{sys})$  GeV with the Template method and  $m_t = 177.5 \pm 5.8(\text{stat}) \pm 7.1(\text{sys})$  GeV with the Ideogram method. The dominant systematic uncertainty comes from jet energy scale corrections.

### 1.3.3 Single Top Production

The single top quark production cross section is directly proportional to  $|V_{tb}|^2$  (in the absence of any new physics and anomalous couplings of the top quark) and hence can provide a direct measurement of the CKM matrix element  $|V_{tb}|$  and a verification of the unitarity of the CKM matrix.

Single top production through the electroweak processes of virtual W exchange ( $p\bar{p} \rightarrow t\bar{b} + X$ ) ( $s$ -channel) and W-gluon fusion ( $p\bar{p} \rightarrow tq\bar{b} + X$ ) ( $t$ -channel) has not yet been observed. A search has been performed using a sample of  $164 \text{ pb}^{-1}$ . Events with one high  $p_T$  electron (muon) with  $p_T > 15$  GeV and  $|\eta| < 1.1$  ( $|\eta| < 2.0$ ),  $E_T > 15$  GeV and between 2 and 4 jets with  $E_T > 15$  GeV, and  $|\eta| < 3.4$  and with the leading jet having  $E_T > 25$  GeV and  $|\eta| < 2.5$ . In addition, at least one jet is required to be b-tagged. The backgrounds arise from W/Z+jets production,  $t\bar{t}$  and QCD multijet events. A 95% C.L. upper limit on the cross section of  $\sigma_t < 23$  pb has been extracted for the sum of the cross sections in the  $s$ - and  $t$ - channels, assuming their ratios to be as predicted by the SM. It is expected that with about  $1 \text{ fb}^{-1}$  of data, observation of the single top production at a  $5\sigma$  level will be possible.

### 1.4. Summary and prospects

Fermilab Run II is progressing very well; the accelerator upgrades for Run II are providing continually improving luminosity performance, with  $670 \text{ pb}^{-1}$  delivered to each experiment so far. With a data set about four times larger than that collected in Run I already in hand, the era of precision measurements has begun at the Tevatron collider experiments. The DØ detector is performing well and many important physics results are emerging from the Run II data. The preliminary results presented here on W and Z boson and di-boson production cross sections in leptonic channels are consistent with Standard Model expectations. The top pair production cross section has been measured using *dilepton* and *lepton+jets* channels which are in agreement with the SM prediction of  $6.7_{-0.9}^{+0.7}$  pb. Measurements of the top quark mass using *lepton+jets*

events are consistent with measurements from Run I. A limit on the single top production cross section has been set. As yet, there are no signs of new physics.

In a couple of years, about  $2 \text{ fb}^{-1}$  of data will be available. With this data set, the W mass will be measured within an uncertainty of 30 MeV and the top quark mass will be known to within 2 GeV. These two measurements, coupled with the precision electroweak results, will provide a tighter constraint on the mass of the SM Higgs boson. The error on the top pair production cross section, which is now about 30% will be reduced to about 10%. Single top quark production will likely be observed, which itself would be a major achievement, and  $|V_{tb}|$  will be measured to about 10% precision. These and other electroweak and top physics measurements will not only provide a rich harvest of Standard Model physics but also might bring into view some hints of new physics beyond the Standard Model.

### 1.5. Acknowledgements

I would like to thank my DØ collaborators, in particular Dmitri Denisov, Ia Iashvili, Aurelio Juste, Lisa Shabalina and Marco Verzocchi for their invaluable input during the preparation of this talk. Fermilab is operated by the Universities Research Association Inc., under contract number DE-AC02-76CH03000 with the U.S. Department of Energy.

### References

1. CDF Collaboration, F. Abe *et al.*, *Phys. Rev. Lett.*, **74**, 2626 (1995); DØ Collaboration, S. Abachi, *et al.*, *Phys. Rev. Lett.*, **74**, 2632 (1995); For a comprehensive review of top quark physics at the Tevatron, see P.C. Bhat, H.B. Prosper and S.S. Snyder, *Int. J. Mod. Phys. A***13**, 5113 (1998).
2. P.C. Bhat and W.J. Spalding, FERMILAB-CONF-04-280-AD, hep-ex/04100046, To be published in the Proceedings of the 15<sup>th</sup> Topical Conference on Hadron Collider Physics, HCP2004, Michigan State University, East Lansing, MI, June 14-18, 2004 (AIP, NY, 2004).
3. The DØ Collaboration, V. Abazov *et al.*, in preparation for submission to *Nucl. Instrum. Methods Phys. Res. A*; T. LeCompte and H.T. Diehl, *Ann. Rev. Nucl. Part. Sci.* **50**, 71 (2000).
4. T. Sjöstrand *et al.*, *Comput. Phys. Commun.*, **135**, 238 (2001).
5. The DØ Collaboration, *Phys. Rev. D.*, **58**, 052001 (1998); *Phys. Rev. D.*, **67**, 012004 (2003).
6. The DØ Collaboration, *Nature* **429**, 638 (2004) and references therein; "Combination of CDF and DØ results on the top quark mass," The CDF and DØ Collaborations and Tevatron Electroweak Group, hep-ex/0404010.